Paleoceanography and Paleoclimatology

RESEARCH ARTICLE
10.1029/2020PA004148

Key Points:

- Persistent meridional gradient in dust deposition implies no large southward shift of intertropical convergence zone at the Last Glacial Maximum
- Last glacial/late-Holocene dust flux ratios vary with latitude, suggesting seasonal differences in glacial dust emission and deposition
- Terrigenous fluxes from South America dominate in the western tropical Atlantic, reaching hundreds of kilometers into the open ocean

Supporting Information:

- Supporting Information S1
- Data Set S1

Correspondence to:
G. H. Rowland,
gr1850@bristol.ac.uk

Citation:
Rowland, G. H., Robinson, L. F., Hendry, K. R., Ng, H. C., McGee, D., & McManus, J. F. (2021). The spatial distribution of aeolian dust and terrigenous fluxes in the tropical Atlantic Ocean since the Last Glacial Maximum. *Paleoceanography and Paleoclimatology*, *36*, e2020PA004148. https://doi.org/10.1029/2020PA004148

Received 10 OCT 2020
Accepted 17 DEC 2020

The Spatial Distribution of Aeolian Dust and Terrigenous Fluxes in the Tropical Atlantic Ocean Since the Last Glacial Maximum

George H. Rowland[1], Laura F. Robinson[1], Katharine R. Hendry[1], Hong Chin Ng[1], David McGee[2], and Jerry F. McManus[3]

[1]School of Earth Sciences, University of Bristol, Bristol, UK, [2]Department of Earth, Atmospheric and Planetary Sciences, Massachusetts Institute of Technology, Cambridge, USA, [3]Department of Earth and Environmental Sciences, Lamont-Doherty Earth Observatory of Columbia University, Palisades, NY, USA

Abstract The flux of terrestrial material from the continents to the oceans links the lithosphere, hydrosphere, and biosphere through physical and biogeochemical processes, with important implications for Earth's climate. Quantitative estimates of terrigenous fluxes from sources such as rivers, aeolian dust, and resuspended shelf sediments are required to understand how the processes delivering terrigenous material respond to and are influenced by climate. We compile thorium-230 normalized ^{232}Th flux records in the tropical Atlantic to provide an improved understanding of aeolian fluxes since the Last Glacial Maximum (LGM). By identifying and isolating sites dominated by aeolian terrigenous inputs, we show that there was a persistent meridional gradient in dust fluxes in the eastern equatorial Atlantic at the LGM, arguing against a large southward shift of the intertropical convergence zone during LGM boreal winter. The ratio of LGM to late-Holocene ^{232}Th fluxes highlights a meridional difference in the magnitude of variations in dust deposition, with sites <10°N showing larger changes over time. This supports an interpretation of increased trade wind strength at the LGM, potentially combined with differential changes in soil moisture and reductions in higher altitude summer winds. Our results also highlight the persistent importance of continental margins as sources of high terrigenous flux to the open ocean. This is especially evident in the western tropical Atlantic, where study locations reveal the primary influence of the South American continent up to >700 km away, characterized by ^{232}Th fluxes approximately twice as large as aeolian-dominated sites in the east.

Plain Language Summary The movement of dust and sediment ("detritus") by winds, rain, and rivers, from land to the oceans is affected by Earth's climate. Measurements of past amounts of detritus can help us understand how the processes that move detritus have changed. We collected published measurements of two types of the element thorium from sediments in the tropical Atlantic Ocean dating back to the last ice age (20,000 years ago). The two types of thorium have different sources—seawater and detritus—and allow us to calculate the accumulation of detritus through time. We show that the pattern of desert dust near the equator did not change much between recent times and the peak of the last ice age, suggesting that the monsoon rains—which wash a lot of dust from the atmosphere—were also in the same position. During the peak of the ice age, we found larger changes in detritus at sites that receive most dust in the wintertime nearer the equator, which suggests that, on the whole, winds strengthened more in that season. We also traced large amounts of detritus from South America far into the ocean, showing that river-borne detritus can travel hundreds of kilometers from land.

1. Introduction

1.1. Lithogenic Fluxes: Relevance to Climate

Lithogenic fluxes from continents to the oceans depend on climatic processes, such as wind and precipitation, and exert influence on climate through radiative and biogeochemical processes. Radiative effects include the interaction of mineral dust with incoming and outgoing radiation (Evan et al., 2009; Kohfeld & Harrison, 2001; Maher et al., 2010), and the provision of cloud condensation nuclei, which affects albedo (DeMott et al., 2003). These dust properties are thought to influence atmospheric and ocean surface temperatures, and the monsoon systems (Evan et al., 2009; Strong et al., 2015; Williams et al., 2016). Lithogenic

material is a key component in oceanic biogeochemical cycling (Jeandel & Oelkers, 2015), as its dissolution helps to balance alkalinity lost due to carbonate burial (e.g., Broecker & Peng, 1982), and provides nutrients that support primary production (Jeandel & Oelkers, 2015; Moore et al., 2013). The addition of dust to the surface ocean may enhance primary productivity (Jickells & Moore, 2015; Moore et al., 2013; Pabortsava et al., 2017) and increase organic carbon export to the deep ocean (Pabortsava et al., 2017; van der Jagt et al., 2018).

1.2. Lithogenic Fluxes in the Tropical Atlantic

The tropical Atlantic Ocean is an area well suited to the study of terrigenous fluxes from aeolian sources. Northwest Africa lies to the east and is the largest global source of mineral dust, with estimates of the total emission of dust ranging from ~440 to 3,220 Tg/yr (Wu et al., 2020). Satellite-derived and model-derived dust flux estimates indicate 182–260 Tg/yr is transported from Northwest Africa toward the tropical Atlantic Ocean (Ridley et al., 2012; Yu et al., 2015). Dust transport across the Atlantic is highly seasonal (Engelstaedter et al., 2006); most summer dust is transported between ~5°N and 25°N, predominantly at high atmospheric levels (~4–5 km, Ridley et al., 2012), in part due to the thick atmospheric boundary layer resulting from summer insolation (Ben-Ami et al., 2009; Schepanski et al., 2009a). Dust lifted to these high levels is transported west by the African Easterly jet (AEJ) (Nicholson, 2009; Pye, 1987; Wu et al., 2009). In contrast, winter dust is delivered further south (~5°S–15°N), and at lower atmospheric levels (generally <2 km, Ridley et al., 2012) due to reductions in the speed of easterly winds above ~1.5 km (Schütz, 1980) and the strong near-surface northeasterly trade winds, that reach their peak speed during this season (Engelstaedter et al., 2006). This seasonal migration in the position of the dust plume is directly linked to the position of the intertropical convergence zone (ITCZ; Engelstaedter et al., 2006). On longer time scales African dust responds to millennial-scale and orbital-scale climate changes, with increases in dust corresponding to reduced boreal summer insolation and Northern Hemisphere cold events (McGee et al., 2013; Middleton et al., 2018; Mulitza et al., 2008; Skonieczny et al., 2019; Williams et al., 2016).

Large rivers drain into the western tropical Atlantic from South America (Peucker-Ehrenbrink, 2009); the suspended sediment load of the Amazon river alone accounts for an estimated ~750 Tg/yr (Peucker-Ehrenbrink, 2018), suggesting that the fluxes of lithogenic material to the tropical Atlantic from the east (dust) and west (riverine material) are of the same order of magnitude. The resuspension and movement of sediment from continental shelves and slopes provides an additional flux of terrigenous material into the ocean interior (Biscaye & Eittreim, 1977; Wynn et al., 2002). There is evidence that terrigenous fluxes from the Amazon are deposited across the western tropical Atlantic, as recorded in sediment core sites west of the Mid-Atlantic Ridge (François & Bacon, 1991; Hemming et al., 1998; Rühlemann et al., 2001; Zabel et al., 1999). Large changes in the proportion and flux of terrigenous material delivered to these sites since the Last Glacial Maximum (LGM) have been attributed to the effect of sea-level on the position of the continental shelf edge (François & Bacon, 1991; Hemming et al., 1998; Rühlemann et al., 2001). Widespread nepheloid layers and mass wasting at shelf edges (Hemming et al., 1998) alongside changes in ocean currents may have played a role in the distribution of terrigenous fluxes during the LGM (Rühlemann et al., 2001).

1.3. The Position of the ITCZ

The location of the ITCZ across the Atlantic is linked to the position of the tropical rain belt, monsoon systems on South America and Africa, ocean surface salinity, Atlantic Meridional Overturning Circulation (AMOC), and river runoff (Donohoe et al., 2013; Haug et al., 2001; Krebs & Timmermann, 2007; Portilho-Ramos et al., 2017; Schneider et al., 2014). It also manifests as a biogeochemical barrier in the surface ocean, influencing patterns of nitrogen fixation and nutrient limitation (Schlosser et al., 2014). The ITCZ migrates north and south as a response to changes in the energy balance between the hemispheres (Schneider et al., 2014), and its present mean position north of the equator results from the northward heat flux across the equator from the AMOC (Marshall et al., 2014; McGee et al., 2014; Schneider et al., 2014). Thus, constraining the position of the ITCZ through time is important for understanding a range of climate processes.

Latitudinal migrations and effective expansions/contractions of the rain belt may have occurred in the past, the type of change depending on the forcing mechanism (e.g., orbital variations vs. high-latitude freshwater input), and whether or not the ITCZ overlies land or ocean (Singarayer et al., 2017). Changes in the position of the global ITCZ have been hypothesized during periods of past climate change (Arbuszewski et al., 2013; Haug et al., 2001; Jacobel et al., 2016, 2017; McGee et al., 2014; Muller et al., 2012; Wang et al., 2006). In the western tropical Atlantic, there seems to be consensus that during strongly hemispherically asymmetric climate shifts, such as those occurring during Heinrich stadials, the ITCZ could have shifted by several degrees latitude (Broccoli et al., 2006; Burckel et al., 2015; Crivellari et al., 2018; Deplazes et al., 2013; Häggi et al., 2017; Mulitza et al., 2017; Portilho-Ramos et al., 2017; Stríkis et al., 2018; Waelbroeck et al., 2018; Zhang et al., 2015). However, the longer time scale behavior of the ITCZ from LGM to late-Holocene remains less certain.

In the Atlantic region, two proxy-based approaches yield contrasting views of the differences between LGM and late-Holocene precipitation patterns and the past location of the ITCZ. Planktonic foraminiferal $\delta^{18}O$ and Mg/Ca data from cores at the southern edge of the modern ITCZ indicate large (several degrees) latitudinal migrations of the rain belt (Arbuszewski et al., 2013). In contrast, sediment records of n-alkane $\delta^{13}C$ close to Africa indicate a contracted region of C3 plants north and south of the equator during the LGM and Heinrich stadial 1 (HS1) (Collins et al., 2011), implying a contracted rain belt during these times. Both proxies have their own uncertainties, and there are limitations relating to the location and temporal resolution of the sediment cores, such that placing a robust constraint on the ITCZ position through time with the available data is challenging.

As the delivery of aeolian dust may be controlled in large part by wet deposition associated with the ITCZ, reconstructions of past dust fluxes have been applied as one approach for reconstructing shifts in the Pacific ITCZ (Jacobel et al., 2016; McGee et al., 2007; Reimi et al., 2019); no such attempt has yet been made for the Atlantic ITCZ. To reconcile the existing proxy-based estimates (Arbuszewski et al., 2013; Collins et al., 2011) with the model results (Singarayer et al., 2017), we use compiled ^{232}Th flux data to assess whether there is evidence for large latitudinal migrations of the ITCZ over the LGM to late-Holocene transition.

1.4. Approach of This Study

Earlier compilations of terrigenous flux in the tropical Atlantic (Kohfeld & Harrison, 2001) relied on terrigenous fluxes derived from age-model-based mass accumulation rates (e.g., Ruddiman, 1997) which are subject to biases due to sediment redistribution at the seafloor (François et al., 2004). More recently Kienast et al. (2016) generated an improved compilation, combining ^{230}Th normalization (Costa et al., 2020; François et al., 2004) with measurements of lithogenic ^{232}Th for late-Holocene and LGM time slices.

In this study, we build on this latter approach, bringing together temporally and spatially resolved ^{230}Th-normalized records of ^{232}Th accumulation in the tropical Atlantic throughout the last ~25 ka. This new compilation draws on records that reflect aeolian input to the ocean as well as riverine and shelf/slope fluxes. The compilation includes four records that have not been previously considered in the context of terrigenous inputs (Ng et al., 2018). Together these records allow us to divide the study area into broad zones based upon the likely dominant source of ^{232}Th fluxes (i.e., riverine, shelf, or aeolian). We use the data to identify and interpret records that reflect ^{232}Th delivery predominantly from aeolian dust throughout the past ~25 ka. This allows us to determine the past meridional gradients of aeolian dust in the tropical Atlantic at increased spatial and temporal resolution, and to investigate the past position of the ITCZ in the area.

2. Materials and Methods

2.1. Terrigenous Fluxes From ^{230}Th Normalization of ^{232}Th

Thorium-230 normalization (Costa et al., 2020; François et al., 2004; Henderson & Anderson, 2003) relies on the assumption that the flux of ^{230}Th delivered by settling sediment to the seafloor can be predicted. This assumption has been validated by observations and modeling (Bacon, 1984; Hayes et al., 2015; Henderson et al., 1999; Yu et al., 2001). The method is considered to represent a significant improvement on the

traditional approach using fluxes derived from bulk accumulation rates (Costa & McManus, 2017; Costa et al., 2020; François et al., 2004) and generally compares well with other constant-flux proxies, such as ^{3}He, where the two have been measured in the same sediments (e.g., McGee et al., 2010b). One exception is in the presence of intense hydrothermal scavenging regimes where the differences in sediment flux can be large (Lund et al., 2019) over limited spatial scales (Middleton et al., 2020).

The separation and analysis of ^{230}Th and U-series isotopes from the sediment—typically by anion-exchange chromatography and inductively coupled plasma mass spectrometry, ICP-MS—also allows for the measurement of the primordial isotope ^{232}Th. Thorium-232 is preferentially incorporated into melt phases during the processes of crustal formation (Blundy & Wood, 2003), and so is present in high concentrations in the continental crust—over an order of magnitude greater than in oceanic basalts (Kienast et al., 2016, and references therein; McGee et al., 2007, 2016). This fractionation allows the flux of ^{232}Th recorded in sediments to be used as a proxy for varying terrigenous inputs through time (Adkins et al., 2006; Anderson et al., 2006; Jacobel et al., 2017; McGee et al., 2007; Pourmand et al., 2004). Although it is possible to estimate an absolute flux of lithogenic sediment based on the ^{232}Th concentration of the material in question, this estimate is dependent on the grain size and provenance of the material (e.g., ~14 μg g^{-1} in fine aeolian dust vs. ~11 μg g^{-1} in average upper continental crust; McGee et al., 2016; Rudnick & Gao, 2003; Taylor & McLennan, 1995). We present reconstructions of lithogenic fluxes as ^{232}Th fluxes to avoid a priori assumptions about the source of the material. We note that the term "terrigenous" properly refers to material derived from the continents, while "lithogenic" and "detrital" suggest material derived from the solid lithosphere (i.e., rocks). However, given the enrichment of ^{232}Th in continental material and the lack of large volcanic inputs to our study sites, in this paper, we use these terms interchangeably.

2.2. Data Compilation

We compiled down-core U and Th isotopic data from the tropical Atlantic that provide a temporal resolution higher than late-Holocene and LGM time slices (e.g., Kienast et al., 2016). The compilation consists of data that were mainly derived from ICP-MS measurements, but also contains data that were obtained with alpha spectrometry (e.g., Francois et al., 1990). The data set covers the last deglacial transition, with the highest data density being between 0 and 18 ka. The 36 cores span a spatial range from 4°S to 31°N latitude, 11°W to 78°W longitude, and 965–5,104 m water depth (Table S1). The sediment core records from McGee et al. (2013) are presented as ^{232}Th fluxes, rather than dust flux as estimated in the original study, to allow for direct comparison to neighboring cores. Fluxes of ^{232}Th from cores KN207-2-GGC6 and KN207-2-GGC3 at the Mid-Atlantic Ridge were normalized to ^{3}He, rather than ^{230}Th (Middleton et al., 2016, 2018).

The data in previous studies were presented in a range of different formats; in some cases, only the raw data were presented, and in other cases, the corrections necessary for ^{230}Th normalization were already undertaken. Our approach here was to use $^{230}Th_{xs}^{0}$ (excess ^{230}Th corrected for the time since deposition and for activity supported by U in the sediment) from the original studies where available. If necessary, the $^{230}Th_{xs}^{0}$ values were recalculated based on the methods set out by Francois et al. (2004), using chronology and correction factors given in the original studies (e.g., ^{238}U/^{232}Th in detrital material) and using the ^{230}Th half-life of Cheng et al. (2000) (Table S1).

2.2.1. Sources of Uncertainty

Analytical uncertainties were taken from the original studies where presented, or given as 2 standard deviations from the mean where fluxes were calculated in this study. These uncertainties are typically smaller than that associated with predicting the vertical ^{230}Th flux (±30%–40%; Costa et al., 2020, and references therein). No specific uncertainty was available for the data from Francois et al. (1990), but an average counting precision of ~8% for ^{230}Th and ^{232}Th (2SD) was reported. In addition, uncertainties associated with the ^{238}U/^{232}Th activity ratios were propagated in the calculation of $^{230}Th_{xs}^{0}$ made in this study using the ratio and corresponding uncertainty provided by the original studies.

In settings with a high proportion of lithogenic material, ^{230}Th-normalized fluxes are sensitive to the assumed value of ^{238}U/^{232}Th in detrital material (Missiaen et al., 2018). The ^{238}U/^{232}Th ratios can vary between

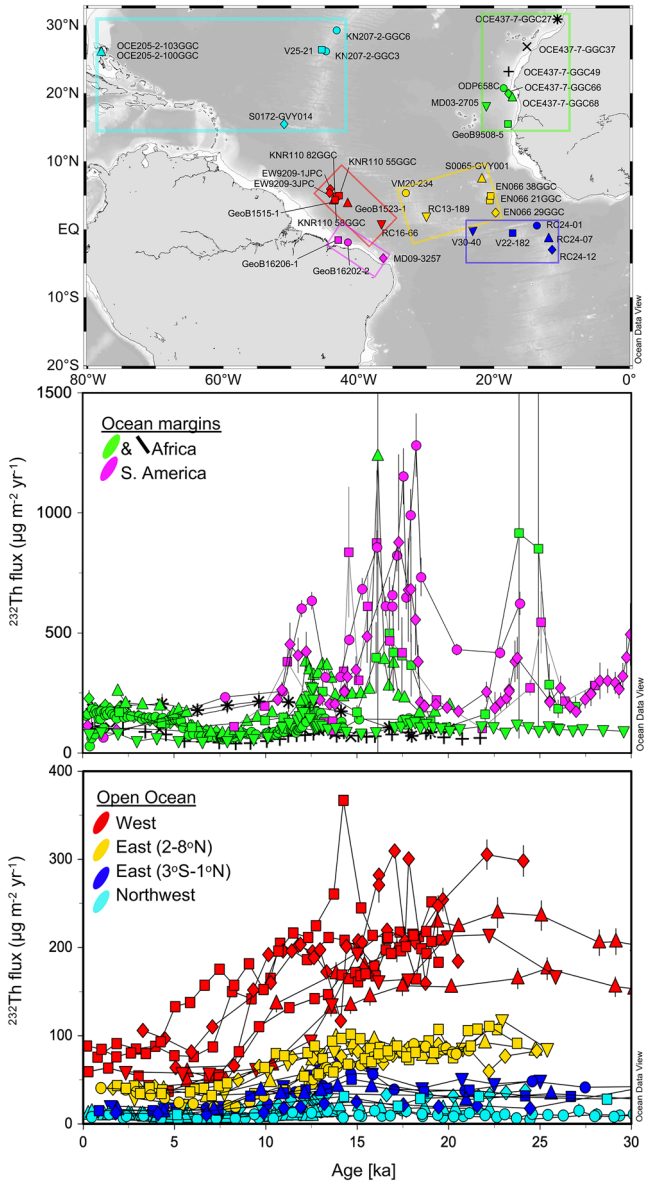

Figure 1. Sediment cores with $^{232}Th/^{230}Th$ data compiled in this study, grouped by ^{232}Th flux magnitude and location. Ocean margin sites are colored green and black (African) and pink (South American), open-ocean sites are colored red ("West"), yellow and blue (East), and cyan ("Northwest") (Adkins et al., 2006; Bradtmiller et al., 2014, 2007; Burckel et al., 2015; François et al., 1990; Lippold et al., 2011, 2012a, 2012b, 2016; McGee et al., 2013; Meckler et al., 2013; Middleton et al., 2016, 2018; Mulitza et al., 2017; Ng et al., 2018; Skonieczny et al., 2019; Voigt et al., 2017; Waelbroeck et al., 2018; Williams et al., 2016). Some closely spaced cores from a particular study are given the same symbols. Error bars are 2SD if calculated here, or as given by the original studies. No uncertainty is plotted for the data from Francois et al. (1990) (as discussed in the text). Figure created using Ocean Data View (Schlitzer, 2018).

source lithologies (Costa et al., 2020, and references therein), but measurements of African dusts and Amazon river sediments (i.e., the major terrigenous sources for our study area) indicate similar average values of $^{238}U/^{232}Th$ (0.83 ± 0.1 and 0.75 ± 0.1, respectively, activity ratio ±1σ; Bouchez et al., 2011; Muhs et al., 2007). Records at the ocean margins with high proportions of terrigenous material must be more cautiously interpreted than those in open-ocean settings with lower lithogenic content. For example, core GeoB16206-1 (South American margin, magenta square, Figure 1; Voigt et al., 2017) records ^{232}Th flux from 93 to 875 µg m^{-2} yr^{-1} with $^{238}U/^{232}Th$ activity ratio = 0.4, which increases to 99–2,332 µg m^{-2} yr^{-1} (7%–167% change) with $^{238}U/^{232}Th$ = 0.5. Some original studies analyzing closely spaced records used different detrital $^{238}U/^{232}Th$ or other correction factors in the calculation of $^{230}Th_{xs}{}^{0}$ (Table S1 and Figure S1). Biases in ^{232}Th fluxes are most likely at the Ceará Rise ("West" core group, Figure 1) and around the African Margin, where differences of 0.13 and 0.2 in the assumed $^{238}U/^{232}Th$ ratio between closely spaced cores are coupled with high lithogenic proportions (i.e., >50%). However, reprocessing data from cores 1JPC and 3JPC (red diamonds, "West" core group, Figure 1; Ng et al., 2018) using a lower detrital $^{238}U/^{232}Th$ of 0.47 (Lippold et al., 2016; Figure S1) we find an average difference in ^{232}Th fluxes of only 5% and 15% for 1JPC and 3JPC, respectively (maximum ~20%). This suggests that for mid-ocean cores with moderately high lithogenic contents the impact of different assumed lithogenic $^{238}U/^{232}Th$ ratios is less than other uncertainties inherent to the ^{230}Th normalization technique (Costa et al., 2020).

The age control on the different sedimentary records varies in resolution and quality (Table S1). Eighteen cores have ages constrained by ^{14}C dates on planktic foraminifera. Other chronologies use $\delta^{18}O$ correlation that is dependent on uncalibrated ^{14}C dates (François et al., 1990; Table S1) and an assumed core-top age of zero (inconsistent with ^{14}C dated core-top ages >3 ka; e.g., Ng et al., 2018). As such there are systematic offsets in the chronologies of some cores (François et al., 1990; ~2–4 ka, Table S1). We reduce the significance of uncertainty from any single record by focusing on multimillennial-scale changes and the main regional trends. This approach is suited to the setting of many open-ocean cores with low sedimentation rates where millennial-scale variations may have been masked by bioturbation (Middleton et al., 2018; Williams et al., 2016).

3. ^{232}Th Fluxes in the Tropical Atlantic Since the LGM

3.1. Ocean Margin Data

Sediment cores recovered from both eastern and western margins of the tropical Atlantic show significantly higher ^{232}Th fluxes than those from the open ocean. The sites defined here as margin records are located within 300 km of the nearest coast, except for core MD03-2705 (Skonieczny et al., 2019), which is located >500 km. This site is considered to be transitional as it exhibits ^{232}Th fluxes similar to both margin and open-ocean sites at different times. The margin sites generally have ^{232}Th fluxes >200 µg m^{-2} yr^{-1} and show high temporal variability, particularly during the deglaciation (Figure 1). In African margin cores, there is often a peak in ^{232}Th fluxes around the 12–13 ka (associated with the Younger Dryas) and variably expressed peaks during Heinrich Stadials 1 and 2 (cf. cores

ODP658C and OCE437-7-GC68 with GeoB9508-5 and MD03-2705). The relative magnitude of these flux peaks is different between cores (Figure 1). The African margin cores show lower ^{232}Th fluxes during much of the mid-Holocene, with flux minima often around 6–8 ka. Fluxes at the South American continental margin were up to an order of magnitude higher than those on the African margin during the deglaciation; the main peaks are at ~11–13, ~15–18, and ~24–25 ka. Late-Holocene fluxes are lower than LGM fluxes in the two South American records that resolve both time periods (a factor of 1.7× to 6.7× higher at the LGM).

3.2. Open-Ocean Data

Away from the continental margins (beyond ~300 km) the open-ocean records are largely consistent in terms of their broad scale temporal trends. In general, the lowest ^{232}Th fluxes are observed during the mid-Holocene, fluxes during the LGM are relatively elevated, and peak fluxes are typically observed during the deglaciation. These core sites can be further divided into three groups based on the magnitudes and temporal patterns of their ^{232}Th flux (Figure 1).

3.2.1. High ^{232}Th Flux Sites

Eight sites located west of the Mid-Atlantic Ridge but away from the continental slope show the highest ^{232}Th flux among the open-ocean sites (red symbols, Figure 1). The cores all show an interglacial-glacial difference, with average LGM (19–26.5 ka) ^{232}Th fluxes of ~220 ± 40 μg m^{-2} yr^{-1} (1SD), compared to a Holocene (0–10 ka) average of ~90 ± 40 μg m^{-2} yr^{-1}. The initiation and end of the deglacial transition appears to span a range of several thousand years ages between the different records, likely as a result of the variable core chronologies (Table S1).

3.2.2. Moderate ^{232}Th Flux Sites

Six sites on or east of the Mid-Atlantic Ridge from 1.9 to 7.4°N (yellow symbols in Figure 1) have ^{232}Th fluxes of 36 ± 10 μg m^{-2} yr^{-1} in the Holocene and LGM fluxes of 88 ± 13 μg m^{-2} yr^{-1}. These sites also show shorter timescale variations, with peaks in ^{232}Th fluxes around the time of the deglaciation and at the LGM. Minimum values are typically reached in the mid-Holocene, where fluxes remain lower than late-Holocene values for a time period of several thousand years (e.g., core VM20-234; Williams et al., 2016). These sites are at least 840 km from the coast at present, with the LGM coast up to ~200 km closer. The main LGM to Holocene reduction in dust flux is offset by up to several thousand years in the different cores, with the mid-Holocene flux minimum being reached between ~5.4 and 8.4 ka.

3.2.3. Low ^{232}Th Flux Sites

Eleven sites designated as low ^{232}Th flux sites in this study come from the broadest geographical range, with five equatorial cores (Bradtmiller et al., 2007) located around the Mid-Atlantic Ridge (dark blue symbols in Figure 1), and six cores located between 15 and 30°N (cyan symbols in Figure 1). Two cores are included in which ^{232}Th fluxes have been estimated by means of normalization to extra-terrestrial ^{3}He (Middleton et al., 2018). Maximum fluxes are seen around the time of the deglaciation, with the most southerly cores in the group (dark blue symbols in Figure 1) showing peak deglacial values 25–72 μg m^{-2} yr^{-1}, and those further north and west (cyan symbols in Figure 1) showing peak values 15–34 μg m^{-2} yr^{-1}. The low flux sites have minima around the early-Holocene to mid-Holocene. The low ^{232}Th flux sites are all distal from continents (~700–2,800 km), apart from two cores near the Bahamas (Williams et al., 2016), which are ~200 km from the coast of North America.

4. Discussion

4.1. The Influence of Continental Margins

4.1.1. High and Variable Fluxes at Continental Margins

Our compilation shows that the flux of terrigenous material at the ocean margins is much higher (well in excess of 200 μg m^{-2} yr^{-1}) than fluxes to the more remote parts of the ocean (Kienast et al., 2016). The

marked differences between the African margin records (green and black symbols, Figure 1), both in terms of the absolute fluxes and the temporal variability of the records could be explained by the different distances to ^{232}Th sources, variable contributions of riverine or resuspended shelf/slope material, variable susceptibility to bioturbation, differences in aeolian deposition or by age-model biases. Because modeled dust flux gradients are generally gradual—unless some atmospheric barrier acts to rapidly remove dust (Albani et al., 2016; Mahowald et al., 2005)—it is plausible that some of the differences between the closely spaced cores may be attributed to non-aeolian processes. In order to use sites at ocean margins to reconstruct dust fluxes, additional techniques must be used to separate aeolian and hemipelagic or riverine influences (e.g., McGee et al., 2013).

The records at the South American margin (magenta symbols, Figure 1) have been interpreted as representing riverine inputs, with the prominent peaks in some records reflecting precipitation maxima (Waelbroeck et al., 2018). The deglacial peaks are similar to those recorded at the African margin, and are coincident with major millennial climate variations (the Younger Dryas, HS1, and HS2). The co-occurrence of high ^{232}Th fluxes at both margins of the tropical Atlantic during millennial-scale climate events indicates a similar response of lithogenic flux to the atmospheric reorganizations during these climate periods, although different processes dominated at each margin (i.e., riverine input vs. dust) (McGee et al., 2013; Mulitza et al., 2017). It is notable that during these periods of rapid and intense climatic change the terrigenous flux component of the climate system was also at an extreme.

4.1.2. Long Range Transport to the Western Tropical Atlantic

Distal sites as far from continental margins as the Ceará Rise (>600 km from South America) show fluxes far above those of other open-ocean sites ("West" core group, red symbols, Figure 1), similar, on average, to those at the African margin. Kienast et al. (2016) noted the penetration of terrigenous fluxes into this part of the western Atlantic and excluded the sites from their compilation of LGM aeolian deposition. However, the increased temporal resolution in this study shows that the records at the Ceará Rise have been consistently elevated for >25 ka and should also be excluded from Holocene dust reconstructions. We also observe fluxes of this magnitude far from the Amazon river mouth or South American continent (>1,400 and >500 km, respectively; core RC16-66, red inverted triangle, Figure 1; Bradtmiller et al., 2007). This pattern and magnitude of ^{232}Th fluxes indicate that resuspended and/or riverine fluxes from South America have been the dominant source of lithogenic sediment to the western tropical Atlantic throughout the last ~30 ka (Damuth, 1977; François & Bacon, 1991; Hemming et al., 1998; Rühlemann et al., 2001). In the subsequent sections, we focus on distinguishing and interpreting sites that we believe to be dominated by aeolian inputs.

4.2. Aeolian-Dominated Sites

Cores at latitudes <10°N on or east of the Mid-Atlantic Ridge ("East" core groups, yellow and blue symbols, Figure 1), and those at latitudes >10°N, on or west of the Mid-Atlantic Ridge ("Northwest" core group, cyan symbols, Figure 1) are interpreted as being dominated by aeolian deposition. These sites, far from the ocean margins, have substantially lower ^{232}Th fluxes than those at the margins. An African origin for ^{232}Th in some of these cores is supported by Pb isotopic analysis on cores at the Sierra Leone Rise ("East" core group, yellow squares, Figure 1; Abouchami & Zabel, 2003), as well as Nd isotopic evidence, albeit at time-slice resolution (Grousset et al., 1998). Cores close to the African margin that have been corrected for riverine/resuspended inputs (McGee et al., 2013) or show ^{232}Th fluxes similar to more distal sites (Skonieczny et al., 2019) are also considered to reflect aeolian inputs (Section 4.2.2).

4.2.1. Latitudinal Trends of ^{232}Th Flux and the Position of the ITCZ

In order to reconstruct the position of the ITCZ through time we followed the approach applied in the tropical Pacific (Jacobel et al., 2016; McGee et al., 2007). The method assumes that the ITCZ represents a significant barrier to atmospheric dust transport and leads to an additional removal flux of dust (due to the strong precipitation). This assumption is supported by the strong latitudinal gradients in surface ocean dissolved Al and Fe concentrations across the ITCZ (Moore et al., 2009; Schlosser et al., 2014), as well as by

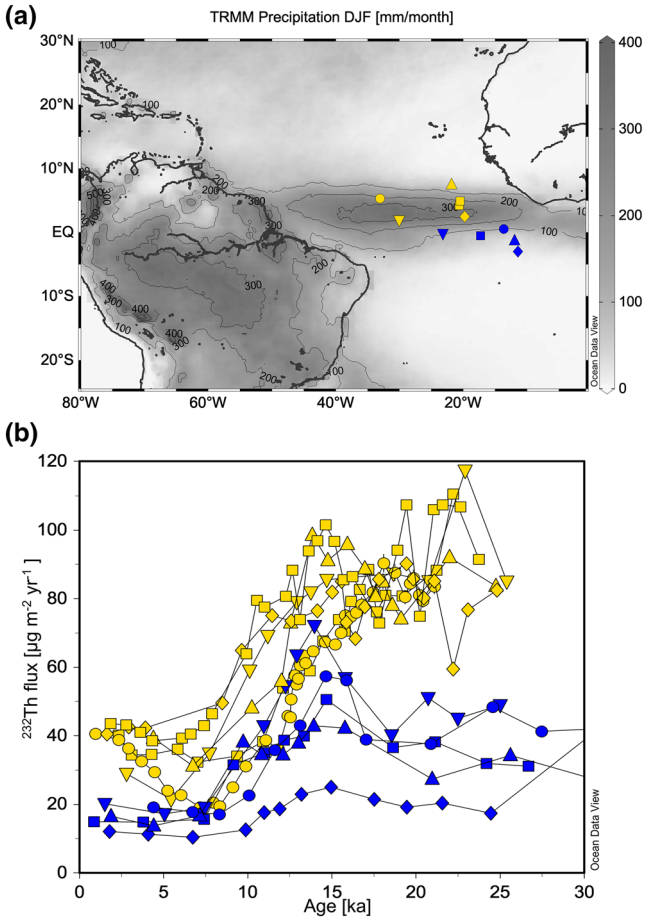

Figure 2. (a) Position of the modern boreal winter ITCZ indicated by the seasonal average (December to February) precipitation rate (greyscale color and contours, maximum values shown are 400 and 300 mm/month, respectively). (b) ^{232}Th flux in sediment cores; sites shown in blue lie approximately south of the ITCZ during modern boreal winter, those shown in yellow approximately underlie the ITCZ during that season. Precipitation data from January 1998 to February 2019 are from the tropical rainfall measuring mission (TRMM; Goddard Earth Sciences Data and Information Services Center (GES DISC), 2011), accessed through the Giovanni online data system. ITCZ, intertropical convergence zone. Figure created using Ocean Data View (Schlitzer, 2018).

modeled and observed associations between precipitation and dust deposition (van der Does et al., 2020; Yu et al., 2019). This wet deposition in the ITCZ results in a steeper gradient of dust deposition (with latitude) at the southern edge of the dust plume than is seen further north, in contrast to the approximately symmetrical pattern of aerosol thickness indicated by satellite retrievals (Yu et al., 2019). Under a scenario with a shift in position of the ITCZ, the associated strong gradient in dust deposition would move concurrently (e.g., a southward shift in the ITCZ would also be expected to move the strong gradient in dust deposition further south).

We focused on sediment cores from the eastern tropical Atlantic that are likely to be sensitive to shifts in the ITCZ and have minimal sensitivity to additional factors, such as distance from the dust sources or the seasonality of dust deposition. These sites receive dust dominantly during boreal winter (Yu et al., 2019) and span a latitudinal gradient across the position of the present boreal winter ITCZ. The relatively low total accumulation rates in open-ocean cores do not allow examination of millennial-scale latitudinal shifts in the ITCZ (such as those thought to occur during Heinrich stadials; e.g., Broccoli et al., 2006). Instead, we focused on assessing evidence for the hypothesized 7° latitudinal shift southward of the LGM ITCZ (Arbuszewski et al., 2013), compared to the late-Holocene.

A prominent feature of the data is a latitudinal gradient in ^{232}Th fluxes in the eastern tropical Atlantic, with higher fluxes in the north (~2.4–7.4°N) and lower fluxes in the south (~0.6–3.0°S) This latitudinal gradient persists at the LGM and the late-Holocene with a north-south reduction in flux of about a factor of 3 (late-Holocene) to 4 (LGM) (Figures 2 and 3). The highest ^{232}Th fluxes occur at approximately the same latitude as the maximum winter precipitation rate. In addition, the highest latitudinal gradient is approximately coincident with the highest latitudinal gradient in precipitation rate (Figure 3). The strong gradient in ^{232}Th flux is thus likely due to the position of the ITCZ at around the same latitude during the LGM and the late-Holocene (Figures 2 and 3). A similar feature is also revealed by a dust deposition model (Albani et al., 2016), which indicates a decrease in dust flux of around a factor of 4.5 (at 21 ka) to 6.5 (at 2 ka) moving south between about 4°N and 1°N (Figure 3). The modeled decrease in dust flux is dominated by the decrease in wet-dust deposition over this latitude (Albani et al., 2014), implying a dominant role for ITCZ processes in scavenging dust from the atmosphere. Although in broad agreement, the modeled dust flux curve indicates a decline in values starting slightly further north than the ^{232}Th flux data.

Some difference between modeled dust and ^{232}Th flux gradients might be expected due to the lateral advection of dust particles by ocean currents (Anderson et al., 2016). However, a significant northward current would be required for the reconstructed latitudinal ^{232}Th flux gradient to be an artifact of such oceanic redistribution. In the modern tropical Atlantic, there is no strong northward current; flow in the surface and subsurface is dominated by zonal currents (Brandt et al., 2006; Schmid et al., 2001; Zhang et al., 2003). The presence of zonal ^{232}Th flux gradients across the tropical Atlantic, despite the strong east-west currents gives us confidence that sediments do capture dust deposition patterns (Anderson et al., 2016; Rowland et al., 2017).

The ^{232}Th flux data support model results that indicate the maximum southern extent of the ITCZ over the Atlantic was similar at the late-Holocene and LGM (Singarayer et al., 2017). The model generally highlights expansion and contraction of the ITCZ seasonal range on orbital time scales over the ocean, rather than large-scale latitudinal shifts of the marine ITCZ. Our results argue against a potential 7° latitudinal shift in the LGM ITCZ (Arbuszewski et al., 2013), as the gradient of ^{232}Th fluxes between the northern and southern

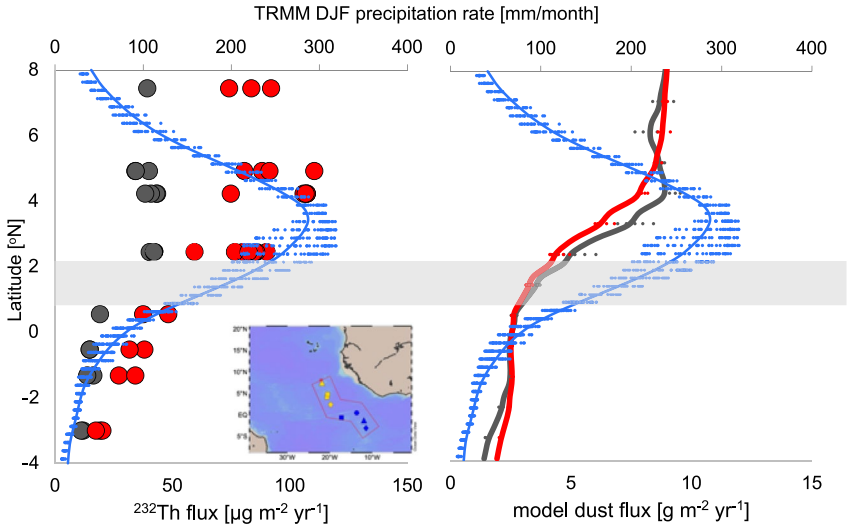

Figure 3. Left: The latitudinal gradient in ^{232}Th fluxes at the late-Holocene (0–5 ka) shown as gray dots, and around the LGM (19–26.5 ka) shown as red dots from a transect of sites (inset map). Right: Modeled dust fluxes for 2 ka (gray dots and line) and 21 ka scenarios (red dots and line) for the same transect from Albani et al. (2016) are shown. Also plotted is the TRMM average precipitation rate for December to February (Goddard Earth Sciences Data and Information Services Center (GES DISC), 2011). The range of latitudes coincident with the highest gradient of ^{232}Th flux and with a high gradient in precipitation rate is highlighted by a gray bar. LGM, Last Glacial Maximum; TRMM, tropical rainfall measuring mission.

sites of the transect is expected to decrease, in relative terms, if the ITCZ dust barrier were shifted so far south. Our data are consistent with no large shift in the mean position of the boreal winter Atlantic ITCZ at the LGM (Singarayer et al., 2017), or in the position of the winter dust plume emanating from the Sahara (Grousset et al., 1998; Sarnthein et al., 1981). At the most, any southward shift in the boreal winter ITCZ at the LGM must have been less than the minimum spatial resolution of our core transect (i.e., <2° latitude). One important consequence of this interpretation is the potential change in the amount of precipitation in the ITCZ during the LGM. If precipitation within the ITCZ was reduced, then dust might be less efficiently scavenged by the ITCZ, as is suggested in the eastern Pacific (McGee et al., 2007). If true, the reduced precipitation would serve to decrease the gradient in dust fluxes. Following this scenario, the gradient in ^{232}Th fluxes that we reconstruct may be a minimum estimate for the gradient in LGM dust loading (e.g., Collins et al., 2011).

During the deglaciation (11–18 ka) the latitudinal gradient in ^{232}Th fluxes appears to break down (in relative terms, Figure 2). The average ^{232}Th flux of all sites further north (73 μg m^{-2} yr^{-1}, yellow symbols Figure 2) is a factor of 1.7 higher than those to the south (42 μg m^{-2} yr^{-1}, blue symbols Figure 2), in contrast to a factor of 2.5 higher during the late-Holocene (0–5 ka, 38 μg m^{-2} yr^{-1}/15 μg m^{-2} yr^{-1}) and LGM (19–26.5 ka, 88 μg m^{-2} yr^{-1}/35 μg m^{-2} yr^{-1}). This reduced latitudinal gradient in ^{232}Th flux and the prominent peaks of ^{232}Th flux observed at the southern sites (Figure 2) would support the notion of a southward shifted ITCZ during the deglaciation (Broccoli et al., 2006; Portilho-Ramos et al., 2017; Singarayer et al., 2017). However, this interpretation is sensitive to age-model uncertainties (Section 2.1.1); systematic offsets in model ages combined with rapid changes in ^{232}Th flux could produce the apparent breakdown of latitudinal gradients.

Throughout the Holocene the north-south gradient in ^{232}Th fluxes persists, with northern sites a factor of 1.8 higher during the early-Holocene (5–10 ka), increasing to a factor of 2.5 at the late-Holocene (average of yellow and blue sites, "East" core groups, Figures 1 and 2). During the early-Holocene the seasonality of northern hemisphere insolation was high, and the ITCZ is thought to have expanded northwards during boreal summer, and further south during boreal winter (Singarayer et al., 2017). Under these conditions, one might expect that the gradient between the northern and southern transect sites to be greatly reduced, because the barrier to dust should have been removed during the season relevant for dust deposition at these sites (boreal winter). There are several nonexclusive scenarios that could contribute to the early-Holocene

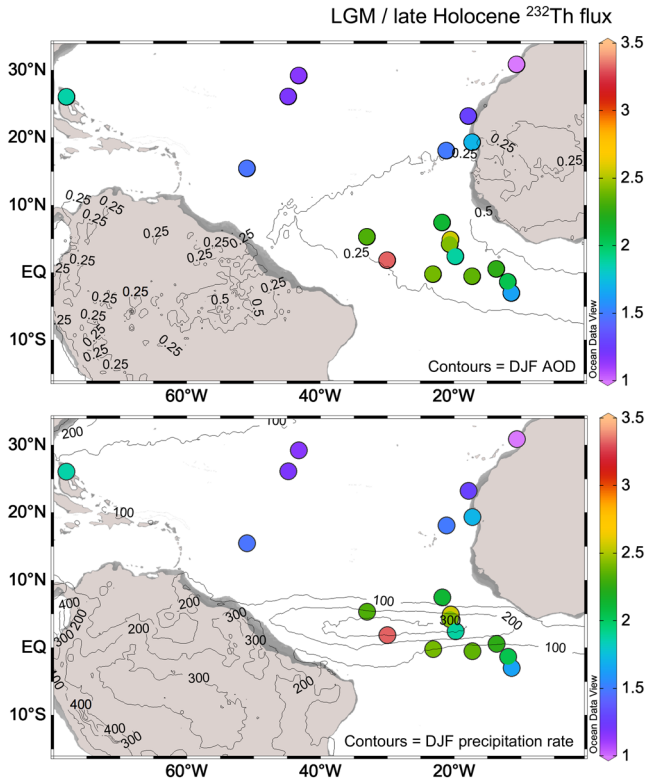

Figure 4. The ratio of LGM (19–26.5 ka) to late-Holocene (0–5 ka) ^{232}Th flux for sites representative of aeolian terrigenous inputs, shown by a color scale. Ratios from three African margin sites of McGee et al. (2013) are calculated using the estimated aeolian flux from that study, rather than bulk ^{232}Th flux. Upper panel contours indicate mean December-February 555 nm aerosol optical depth from the multiangle imaging spectroradiometer for the time period December 2000 to February 2017, using the MIL3MAE version 4 data product (Diner, 2009), and accessed through the Giovanni online data system. Lower panel contours are TRMM December to February precipitation rate (mm/month), the same as the upper panel of Figure 2. LGM, Last Glacial Maximum; TRMM, tropical rainfall measuring mission. Figure created using Ocean Data View (Schlitzer, 2018).

gradient, resulting from atmospheric or postdepositional processes. One explanation for the persistent, albeit reduced, early-Holocene ^{232}Th flux gradient is that the ITCZ may have occupied locations between northern and southern transect sites for sufficient time to scavenge dust during its seasonal transit between the higher latitudinal maxima. The efficiency of dust removal associated with the ITCZ may have been greater during the mid-Holocene, potentially due to higher boreal winter rainfall in the Atlantic rain belt during the mid-Holocene (e.g., Collins et al., 2011). Alternatively, the ^{232}Th-flux gradient may have been maintained if the ITCZ did not shift far enough from its present position to remove the dust barrier between the low ^{232}Th and moderate ^{232}Th sites (in contradiction with model results; Singarayer et al., 2017). Increasing bioturbation with decreasing latitude could also contribute to the north-south gradient by moving the low mid-Holocene ^{232}Th flux signal down-core.

4.2.2. Changes in Aeolian Flux: LGM to Late-Holocene Ratios

Dust fluxes decline more from the LGM to late-Holocene at sites south of ~10°N (Figure 4; Table S2). Sites <10°N show an average change in ^{232}Th fluxes from LGM to late-Holocene of a factor of 2.30 ± 0.26 (n = 11, 2SE), while those >10°N show an average factor of 1.36 ± 0.25 (n = 8, 2SE) difference. Although flux ratios vary between cores within each latitudinal group (Figure 4), the largest differences are explicable by non-aeolian processes and the overall latitudinal pattern of flux ratios is consistent. For example, at the Bahamas site (Williams et al., 2016), the high LGM/late-Holocene ^{232}Th flux ratio, ~1.9, may be explained by additional contributions from North American terrigenous sources (e.g., aeolian dust prevalent during glacial periods), bioturbation of deglacial flux maxima or biases in ^{230}Th normalization (due to the shallow water depth and/or variable sediment focusing; Williams et al., 2016). Likewise, the low flux ratio, <1, in core OCE437-3-GC27 at the African margin may be explained by the high proportion of non-aeolian inputs, high focusing factors and the presence of an active submarine canyon at the site (McGee et al., 2013).

It has been proposed that North African dust emissions are primarily driven by changes in the African monsoon system, closely linked to Northern Hemisphere insolation, rather than glacial-interglacial conditions (Skonieczny et al., 2019). This view is based on the ~240 ka ^{232}Th flux record from core MD03-2705, and is supported by modeled LGM/late-Holocene dust (i.e., glacial/interglacial) flux ratios in the tropical Atlantic ~1 (Albani et al., 2016). However, the high LGM/late-Holocene ^{232}Th flux ratios at open-ocean sites <10°N (~2) align more closely with larger glacial-interglacial shifts in dust fluxes recorded elsewhere (Kienast et al., 2016; Winckler et al., 2008). This discrepancy highlights the question: are the differences in LGM/late-Holocene ^{232}Th flux ratios the result of real latitudinal differences in aeolian processes, or are they an artifact of the sampling sites? Differences in dust emission and wind seasonality, postdepositional changes to the sediment and differences in wet vs. dry dust deposition are all processes that may affect the ^{232}Th flux ratios. Because the latitudinal trend is constrained by a number of cores across a range of depositional environments, we consider real differences in dust emission and deposition with latitude as our favored interpretation. We further discuss the range of possible interpretations below.

One potential artifact associated with the open-ocean records is that bioturbation may affect the LGM/late-Holocene flux ratios. For example, large deglacial peaks in dust deposition (as indicated by margin records; Figure 1) could have been smoothed down-core, artificially elevating LGM ^{232}Th fluxes (Middleton et al., 2018). At individual core sites the sedimentation rate and organic carbon flux determine the efficacy

and the maximum depth of bioturbation, respectively (Mekik & Anderson, 2018; Trauth et al., 1997). Depending on the interplay of each process, higher ^{232}Th flux ratios close to the equator might be explained by higher bioturbation at these more productive sites (Bradtmiller et al., 2007). However, the consistency of flux ratios >10°N between the African margin and mid-ocean, despite vastly different sedimentation regimes, gives us confidence that the pattern of flux ratios represents a real signal (e.g., deglacial and LGM sedimentation rates ~8× higher at the margin; McGee et al., 2013; Middleton et al., 2018). When modeling the effects of bioturbation (Middleton et al., 2018) could not fully account for the differences in LGM/late-Holocene flux changes between margin and open-ocean records. Middleton et al. modeled <4 cm of mixing at their mid-ocean sites >10°N, in good agreement with modern mixing depths of equatorial cores (Trauth et al., 1997). This similarity in mixing depth combined with generally higher sedimentation rates closer to the equator suggests that bioturbation is unlikely to account for the higher ^{232}Th flux ratios at sites <10°N.

The latitudinal differences in relative LGM to late-Holocene ^{232}Th flux change require a physical explanation. Williams et al. (2016) suggested that latitudinal variation in LGM/late-Holocene flux ratios resulted from a southward shift in the ITCZ at the LGM, which we have ruled out. However, the transport efficiency of dust at the LGM may have varied with latitude due to differing impacts of wet and dry deposition with latitude. For example, model results (Albani et al., 2014) indicate a slightly higher proportion of wet deposition at some of the sites <10°N during the LGM compared to the modern, which could contribute to the higher LGM fluxes at these sites. The modeled changes are only ~10% (Figure S2), and many sites do not show any large shift in wet deposition. Changes in LGM rainfall would have a smaller effect at the African margin where dry deposition is generally >80% of the dust flux (Albani et al., 2014; Figure S2). At sites >10°N and >40°W, wet-dust deposition may account for >50% of annual dust flux (Albani et al., 2014; Figure S2). On the other hand, the sensitivity of dust deposition to precipitation in this region may be limited because the dust transport pathway toward these sites is dominated by dry deposition (Albani et al., 2014; Figure S2). Taken together it seems unlikely that changes in rainfall at the LGM could explain the systematic pattern of flux ratios with latitude.

The modern seasonal emission and deposition of dust has a clear variation with latitude (Engelstaeder et al., 2006; Yu et al., 2019), and so the latitudinal difference in LGM/late-Holocene ^{232}Th flux ratios may be linked to dust seasonality during the LGM. The sites <10°N mainly receive dust that is delivered at lower atmospheric levels by the North East trade winds during the boreal winter (Engelstaeder et al., 2006; Yu et al., 2019). In contrast, open-ocean sites at latitudes >10°N receive much of their dust load during the summer (e.g., Ridley et al., 2012). There is some uncertainty regarding the modern dust seasonality for African margin sites >10°N (e.g., GC68, MD03-2705), with sediment traps indicating variable dust flux seasonality, often with a peak during boreal winter (Bory & Newton, 2000; Neuer et al., 1997; Ratmeyer et al., 1999), and more recent satellite studies indicating summer as the primary depositional season (Yu et al., 2015, 2019). These different wind systems and atmospheric features may have different sensitivities to LGM climate changes.

Sarnthein et al. (1981) inferred increases in glacial trade wind strength based on grain-size analysis; upwelling proxies provide equivocal support for this inference (Bradtmiller et al., 2016). Lower-level dust emitted during the winter and carried by the northeast trade winds may be quite sensitive to glacial increases in wind gusts and trade wind strength (McGee et al., 2010a). Glacial increases in key local wind systems, such as the Bodélé low-level jet also likely play a role (Washington et al., 2006). The enhanced glacial low-level wind systems fit with the higher LGM/late-Holocene fluxes at sites <10°N. On the other hand, the atmospheric boundary layer—important for lofting dust to higher atmospheric levels during the summer (Ben-Ami et al., 2009; Engelstaeder & Washington, 2007; Schepanski et al., 2009a)—would presumably have been affected by the slightly lower summer insolation at the LGM (Laskar et al., 2004) and lower temperatures (Peters & Tetzlaff, 1990). In combination with this, a reduction in the wind systems that transport summer dust is also possible at the LGM. For example, the AEJ is dependent on the existence of the meridional temperature gradient between the equator and Sahara (in addition to vegetation cover and other factors; Cook, 1999; Wu et al., 2009). This temperature gradient exists, in part, due to the soil moisture gradient from the equator to the latitude of the Sahara (Cook, 1999). Given modeled reductions in the meridional soil moisture gradient at the LGM (Scheff et al., 2017), the AEJ may well have been weakened at that time, and

there is both model and data support for this possibility. Peters and Tetzlaff (1990) modeled the strength of the AEJ at the LGM and concluded that it was reduced to 65% of its modern strength. Sarnthein et al. (1981) came to a similar conclusion from grain-size analysis of sediments, arguing that easterly wind speeds in the Saharan Air Layer (that approximately encompasses the AEJ; Prospero & Carlson, 1980) were lowered to ~60% of their modern values.

In addition to wind strength, the aridity of dust source areas is a key control of dust emission (McGee et al., 2010a). Although difficult to reconstruct, there is some evidence from proxies and models that different parts of north Africa experienced different changes in soil moisture during the LGM (McGee, 2020; Scheff et al., 2017). The equatorial regions may have had reduced soil moisture at the LGM, with regions further north and northwest showing either little change or potentially showing slightly higher soil moisture and higher moisture availability in lakes (McGee, 2020; Scheff et al., 2017). It is thus plausible that differential changes in dust source surface properties may account for some of the spatial patterns of LGM/late-Holocene flux ratios. For example, sites at the African margin receive significant contributions of winter dust from sources in northwest Africa (Friese et al., 2017), while mid-ocean sites dominated by dust sources further south and east (Schepanski et al., 2009a).

In summary, for certain dust sources the effect of increased LGM surface winds may have been lessened by a modulation of other key processes responsible for the emission (soil moisture), lofting (insolation/temperature), and transport (AEJ strength) of this dust. These combined processes go some way to explaining the lower LGM/late-Holocene flux ratios >10°N, which may be influenced mainly by summer dust (especially at sites far from the African coast). In contrast, those sites <10°N dominated by low-level winter dust would be more sensitive to the increased low-level winds (Sarnthein et al., 1981; Washington et al., 2006) and reduced soil moisture (Scheff et al., 2017) closer to key winter dust sources, such as the Bodélé depression, during the LGM (Engelstaeder et al., 2006; Prospero et al., 2002; Schepanski et al., 2009b). Our data set supports relatively small glacial-interglacial dust flux variability (Skonieczny et al., 2019) for sites >10°N, but we show this conclusion is not supported for sites <10°N and infer a potential role for seasonality in past changes of tropical Atlantic dust flux. Although modeled LGM to late-Holocene dust flux ratios indicate little latitudinal variability over our study region (~0.8–1.2; Albani et al., 2016), they strongly increase between 4°S and 7°S (from ~1 to 4); understanding this discrepancy may be an important avenue for future work.

5. Conclusions

We have compiled published U and Th data from sediment cores to calculate ^{230}Th-normalized ^{232}Th fluxes in order to investigate changes in terrigenous fluxes in the tropical Atlantic throughout the past 25 ka. We have used gradients of late-Holocene and LGM ^{232}Th fluxes at open-ocean sites to test and reject a hypothesis suggesting that the LGM ITCZ was situated several degrees of latitude further south than at present. The strong meridional gradient in LGM ^{232}Th fluxes observed at a similar latitude as during the late-Holocene indicates little change in the boreal winter ITCZ position between these time periods, in line with a recent modeling study (Singarayer et al., 2017) and consistent with small globally averaged ITCZ shifts during the LGM (McGee et al., 2014). The relative change in ^{232}Th flux between the LGM and late-Holocene varies with latitude; sites <10°N have an average LGM/late-Holocene flux ratio of 2.3 (between 1.6 and 3.3), while those >10°N have an average ratio of 1.4 (between 0.7 and 1.9). This difference is potentially linked to the seasonality of dust emission and deposition, with sites dominated by winter-season dust showing larger changes. This pattern, not captured by recent dust models (Albani et al., 2016), may be explained by strengthened trade winds, reductions in higher level summer winds (AEJ), and variable changes in soil moisture since the LGM.

Our compilation also highlights that terrigenous fluxes at continental margins display large amplitude changes, vary on millennial time scales and are orders of magnitude higher than at open-ocean sites. We show that these high, margin-derived, fluxes can propagate far into the open ocean, particularly in the western tropical Atlantic, and that sites in this area should be excluded from comparisons with dust model output throughout the past 25 ka.

Date Availability Statement

Data sets for this research are included in this paper and its supplementary information files and archived in the Mendeley data library (http://dx.doi.org/10.17632/p6sf6wtdvy.1). Data associated with this study are also available from various public databases or the original publications (references are compiled in the caption of Figure 1). The authors declare no financial conflicts of interest.

Acknowledgments
G. H. Rowland was supported by a Natural Environment Research Council studentship (Grant NE/L002434/1). The contribution of J. F. McManus was supported in part by the US-NSF. The authors thank Walter Giebert and David Naafs for helpful discussions.

References

Abouchami, W., & Zabel, M. (2003). Climate forcing of the Pb isotope record of terrigenous input into the Equatorial Atlantic. *Earth and Planetary Science Letters*, *213*(3–4), 221–234. https://doi.org/10.1016/S0012-821X(03)00304-2

Adkins, J., DeMenocal, P., & Eshel, G. (2006). The "African humid period" and the record of marine upwelling from excess 230Th in Ocean Drilling Program Hole 658C. *Paleoceanography*, *21*, PA4203. https://doi.org/10.1029/2005PA001200

Albani, S., Mahowald, N. M., Murphy, L. N., Raiswell, R., Moore, J. K., Anderson, R. F., et al. (2016). Paleodust variability since the Last Glacial Maximum and implications for iron inputs to the ocean. *Geophysical Research Letters*, *43*, 3944–3954. https://doi.org/10.1002/2016GL067911

Albani, S., Mahowald, N. M., Perry, A. T., Scanza, R. A., Zender, C. S., Heavens, N. G., et al. (2014). Improved dust representation in the Community Atmosphere Model. *Journal of Advances in Modeling Earth Systems*, *6*, 541–570. https://doi.org/10.1002/2013MS000279

Anderson, R. F., Cheng, H., Edwards, R. L., Fleisher, M. Q., Hayes, C. T., Huang, K.-F., et al. (2016). How well can we quantify dust deposition to the ocean? *Philosophical Transactions of the Royal Society A: Mathematical, Physical and Engineering Sciences*, *374*(2081), 20150285. https://doi.org/10.1098/rsta.2015.0285

Anderson, R. F., Fleisher, M. Q., & Lao, Y. (2006). Glacial-interglacial variability in the delivery of dust to the central equatorial Pacific Ocean. *Earth and Planetary Science Letters*, *242*, 406–414. https://doi.org/10.1016/j.epsl.2005.11.061

Arbuszewski, J. A., deMenocal, P. B., Cléroux, C., Bradtmiller, L. I., & Mix, A. (2013). Meridional shifts of the Atlantic intertropical convergence zone since the Last Glacial Maximum. *Nature Geoscience*, *6*(11), 959–962. https://doi.org/10.1038/ngeo1961

Bacon, M. P. (1984). Glacial to interglacial changes in carbonate and clay sedimentation in the Atlantic Ocean estimated from 230Th measurements. *Chemical Geology*, *46*(2), 97–111. https://doi.org/10.1016/0009-2541(84)90183-9

Ben-Ami, Y., Koren, I., & Altaratz, O. (2009). Patterns of North African dust transport over the Atlantic: Winter vs. summer, based on CALIPSO first year data. *Atmospheric Chemistry and Physics*, *9*(20), 7867–7875. https://doi.org/10.5194/acp-9-7867-2009

Biscaye, P. E., & Eittreim, S. L. (1977). Suspended particulate loads and transports in the nepheloid layer of the abyssal Atlantic Ocean. *Marine Geology*, *23*(1–2), 155–172. https://doi.org/10.1016/0025-3227(77)90087-1

Blundy, J., & Wood, B. (2003). Mineral-melt partitioning of uranium, thorium and their daughters. In B. Bourdon, G. M. Henderson, C. C. Lundstrom, & S. P. Turner (Eds.), Reviews in mineralogy and geochemistry (52, pp. 59–123). Chantilly, VA: Mineralogical Society of America. https://doi.org/10.2113/0520059

Bory, A. J.-M., & Newton, P. P. (2000). Transport of airborne lithogenic material down through the water column in two contrasting regions of the eastern subtropical North Atlantic Ocean. *Global Biogeochemical Cycles*, *14*(1), 297–315. https://doi.org/10.1029/1999GB900098

Bouchez, J., Gaillardet, J., France-Lanord, C., Maurice, L., & Dutra-Maia, P. (2011). Grain size control of river suspended sediment geochemistry: Clues from Amazon River depth profiles. *Geochemistry, Geophysics, Geosystems*, *12*, Q03008. https://doi.org/10.1029/2010GC003380

Bradtmiller, L. I., Anderson, R. F., Fleisher, M. Q., & Burckle, L. H. (2007). Opal burial in the equatorial Atlantic Ocean over the last 30 ka: Implications for glacial-interglacial changes in the ocean silicon cycle. *Paleoceanography*, *22*, PA4216. https://doi.org/10.1029/2007PA001443

Bradtmiller, L. I., McGee, D., Awalt, M., Evers, J., Yerxa, H., Kinsley, C. W., & deMenocal, P. B. (2016). Changes in biological productivity along the northwest African margin over the past 20,000 years. *Paleoceanography*, *31*, 185–202. https://doi.org/10.1002/2015PA002862

Bradtmiller, L. I., McManus, J. F., & Robinson, L. F. (2014). 231Pa/230Th evidence for a weakened but persistent Atlantic Meridional Overturning Circulation during Heinrich Stadial 1. *Nature Communications*, *5*(1), 5817. https://doi.org/10.1038/ncomms6817

Brandt, P., Schott, F. A., Provost, C., Kartavtseff, A., Hormann, V., Bourlès, B., & Fischer, J. (2006). Circulation in the central equatorial Atlantic: Mean and intraseasonal to seasonal variability. *Geophysical Research Letters*, *33*, L07609. https://doi.org/10.1029/2005GL025498

Broccoli, A. J., Dahl, K. A., & Stouffer, R. J. (2006). Response of the ITCZ to Northern Hemisphere cooling. *Geophysical Research Letters*, *33*, L01702. https://doi.org/10.1029/2005GL024546

Broecker, W. S., & Peng, T.-H. (1982). *Tracers in the sea*. New York, NY: Lamont-Doherty Geological Observatory, Columbia University.

Burckel, P., Waelbroeck, C., Gherardi, J. M., Pichat, S., Arz, H., Lippold, J., et al. (2015). Atlantic Ocean circulation changes preceded millennial tropical South America rainfall events during the last glacial. *Geophysical Research Letters*, *42*, 411–418. https://doi.org/10.1002/2014GL062512

Cheng, H., Edwards, R. L., Hoff, J., Gallup, C. D., Richards, D. A., & Asmerom, Y. (2000). The half-lives of uranium-234 and thorium-230. *Chemical Geology*, *169*(1–2), 17–33. https://doi.org/10.1016/S0009-2541(99)00157-6

Collins, J. A., Schefuß, E., Heslop, D., Mulitza, S., Prange, M., Zabel, M., et al. (2011). Interhemispheric symmetry of the tropical African rainbelt over the past 23,000 years. *Nature Geoscience*, *4*(1), 42–45. https://doi.org/10.1038/ngeo1039

Cook, K. H. (1999). Generation of the African Easterly jet and its role in determining West African precipitation. *Journal of Climate*, *12*(5), 1165–1184. https://doi.org/10.1175/1520-0442(1999)012<1165:GOTAEJ>2.0.CO;2

Costa, K. M., Hayes, C. T., Anderson, R. F., Pavia, F. J., Bausch, A., Deng, F., et al. (2020). 230Th normalization: New insights on an essential tool for quantifying sedimentary fluxes in the modern and quaternary ocean. *Paleoceanography and Paleoclimatology*, *35*, e2019PA003820. https://doi.org/10.1029/2019PA003820

Costa, K. M., & McManus, J. (2017). Efficacy of 230Th normalization in sediments from the Juan de Fuca Ridge, northeast Pacific Ocean. *Geochimica et Cosmochimica Acta*, *197*, 215–225. https://doi.org/10.1016/j.gca.2016.10.034

Crivellari, S., Chiessi, C. M., Kuhnert, H., Häggi, C., da Costa Portilho-Ramos, R., Zeng, J.-Y., et al. (2018). Increased Amazon freshwater discharge during late Heinrich Stadial 1. *Quaternary Science Reviews*, *181*, 144–155. https://doi.org/10.1016/J.QUASCIREV.2017.12.005

Damuth, J. E. (1977). Late Quaternary sedimentation in the western equatorial Atlantic. *Geological Society of America Bulletin*, *88*(5), 695. https://doi.org/10.1130/0016-7606(1977)88<695:LQSITW>2.0.CO;2

DeMott, P. J., Sassen, K., Poellot, M. R., Baumgardner, D., Rogers, D. C., Brooks, S. D., et al. (2003). African dust aerosols as atmospheric ice nuclei. *Geophysical Research Letters*, *30*(14), 1732. https://doi.org/10.1029/2003GL017410

Deplazes, G., Lückge, A., Peterson, L. C., Timmermann, A., Hamann, Y., Hughen, K. A., et al. (2013). Links between tropical rainfall and North Atlantic climate during the last glacial period. *Nature Geoscience*, *6*(3), 213–217. https://doi.org/10.1038/ngeo1712

Diner, D. (2009). *MISR level 3 component global aerosol product covering a month HDF-EOS file-version 4 [data set]*. NASA Langley Atmospheric Science Data Center DAAC. https://doi.org/10.5067/terra/misr/mil3mae_l3.004

Donohoe, A., Marshall, J., Ferreira, D., & McGee, D. (2013). The relationship between ITCZ location and cross-equatorial atmospheric heat transport: From the seasonal cycle to the Last Glacial Maximum. *Journal of Climate*, *26*(11), 3597–3618. https://doi.org/10.1175/JCLI-D-12-00467.1

Engelstaeder, S., Tegen, I., & Washington, R. (2006). North African dust emissions and transport. *Earth-Science Reviews*, *79*(1–2), 73–100. https://doi.org/10.1016/J.EARSCIREV.2006.06.004

Engelstaeder, S., & Washington, R. (2007). Atmospheric controls on the annual cycle of North African dust. *Journal of Geophysical Research*, *112*, D03103. https://doi.org/10.1029/2006JD007195

Evan, A. T., Vimont, D. J., Heidinger, A. K., Kossin, J. P., & Bennartz, R. (2009). The role of aerosols in the evolution of tropical North Atlantic Ocean temperature anomalies. *Science*, *324*(5928), 778–781. https://doi.org/10.1126/science.1167404

François, R., & Bacon, M. P. (1991). Variations in terrigenous input into the deep equatorial Atlantic during the past 24,000 years. *Science*, *251*(5000), 1473–1476.

François, R., Bacon, M. P., & Suman, D. O. (1990). Thorium 230 profiling in deep-sea sediments: High-resolution records of flux and dissolution of carbonate in the equatorial Atlantic during the last 24,000 years. *Paleoceanography*, *5*(5), 761–787. https://doi.org/10.1029/PA005i005p00761

François, R., Frank, M., Rutgers van der Loeff, M. M., & Bacon, M. P. (2004). 230 Th normalization: An essential tool for interpreting sedimentary fluxes during the late Quaternary. *Paleoceanography*, *19*, PA1018. https://doi.org/10.1029/2003PA000939

Friese, C. A., Van Hateren, J. A., Vogt, C., Fischer, G., & Stuut, J. B. W. (2017). Seasonal provenance changes in present-day Saharan dust collected in and off Mauritania. *Atmospheric Chemistry and Physics*, *17*(16), 10163–10193. https://doi.org/10.5194/acp-17-10163-2017

Goddard Earth Sciences Data and Information Services Center (GES DISC). (2011). *Tropical rainfall measuring mission (TRMM), (TMPA/3B43) rainfall estimate L3 1 month 0.25 degree x 0.25 degree V7*. Greenbelt, MD: Goddard Earth Sciences Data and Information Services Center (GES DISC). https://doi.org/10.5067/TRMM/TMPA/MONTH/7

Grousset, F. E., Parra, M., Bory, A., Martinez, P., Bertrand, P., Shimmield, G., & Ellam, R. M. (1998). Saharan wind regimes traced by the Sr-Nd isotopic composition of subtropical Atlantic sediments: Last Glacial Maximum vs today. *Quaternary Science Reviews*, *17*(4–5), 395–409. https://doi.org/10.1016/S0277-3791(97)00048-6

Häggi, C., Chiessi, C. M., Merkel, U., Mulitza, S., Prange, M., Schulz, M., & Schefuß, E. (2017). Response of the Amazon rainforest to late Pleistocene climate variability. *Earth and Planetary Science Letters*, *479*, 50–59. https://doi.org/10.1016/j.epsl.2017.09.013

Haug, G. H., Hughen, K. A., Sigman, D. M., Peterson, L. C., & Röhl, U. (2001). Southward migration of the intertropical convergence zone through the holocene. *Science*, *293*(5533), 1304–1308. https://doi.org/10.1126/science.1059725

Hayes, C. T., Fleisher, M. Q., Huang, K.-F., Robinson, L. F., Lu, Y., Cheng, H., et al. (2015). 230Th and 231Pa on GEOTRACES GA03, the U.S. GEOTRACES North Atlantic transect, and implications for modern and paleoceanographic chemical fluxes. *Deep Sea Research Part II: Topical Studies in Oceanography*, *116*, 29–41. https://doi.org/10.1016/j.dsr2.2014.07.007

Hemming, S., Biscaye, P., Broecker, W., Hemming, N., Klas, M., & Hajdas, I. (1998). Provenance change coupled with increased clay flux during deglacial times in the western equatorial Atlantic. *Palaeogeography, Palaeoclimatology, Palaeoecology*, *142*(3–4), 217–230. https://doi.org/10.1016/S0031-0182(98)00069-8

Henderson, G. M., & Anderson, R. F. (2003). The U-series toolbox for paleoceanography. In B. Bourdon, G. M. Henderson, C. C. Lundstrom & S. P. Turner (Eds.), *Uranium Series Geochemistry, Reviews in Mineralogy and Geochemistry* (Vol. 52, pp. 493–531). The Mineralogical Society of America, The Geochemical Society. https://doi.org/10.2113/0520493

Henderson, G. M., Heinze, C., Anderson, R. F., & Winguth, A. M. E. (1999). Global distribution of the 230Th flux to ocean sediments constrained by GCM modelling. *Deep-Sea Research Part I: Oceanographic Research Papers*, *46*(11), 1861–1893. https://doi.org/10.1016/S0967-0637(99)00030-8

Jacobel, A. W., McManus, J. F., Anderson, R. F., & Winckler, G. (2016). Large deglacial shifts of the Pacific intertropical convergence zone. *Nature Communications*, *7*(1), 10449. https://doi.org/10.1038/ncomms10449

Jacobel, A. W., McManus, J. F., Anderson, R. F., & Winckler, G. (2017). Climate-related response of dust flux to the central equatorial Pacific over the past 150 kyr. *Earth and Planetary Science Letters*, *457*, 160–172. https://doi.org/10.1016/j.epsl.2016.09.042

Jeandel, C., & Oelkers, E. H. (2015). The influence of terrigenous particulate material dissolution on ocean chemistry and global element cycles. *Chemical Geology*, *395*, 50–66. https://doi.org/10.1016/J.CHEMGEO.2014.12.001

Jickells, T., & Moore, C. M. (2015). The importance of atmospheric deposition for ocean productivity. *Annual Review of Ecology, Evolution, and Systematics*, *46*(1), 481–501. https://doi.org/10.1146/annurev-ecolsys-112414-054118

Kienast, S. S., Winckler, G., Lippold, J., Albani, S., & Mahowald, N. M. (2016). Tracing dust input to the global ocean using thorium isotopes in marine sediments: ThoroMap. *Global Biogeochemical Cycles*, *30*, 1526–1541. https://doi.org/10.1002/2016GB005408

Kohfeld, K. E., & Harrison, S. P. (2001). DIRTMAP: The geological record of dust. *Earth-Science Reviews*, *54*(1–3), 81–114. https://doi.org/10.1016/S0012-8252(01)00042-3

Krebs, U., & Timmermann, A. (2007). Tropical air–sea interactions accelerate the recovery of the Atlantic Meridional Overturning Circulation after a major shutdown. *Journal of Climate*, *20*(19), 4940–4956. https://doi.org/10.1175/JCLI4296.1

Laskar, J., Robutel, P., Joutel, F., Gastineau, M., Correia, A. C. M., & Levrard, B. (2004). A long-term numerical solution for the insolation quantities of the Earth. *Astronomy & Astrophysics*, *428*(1), 261–285. https://doi.org/10.1051/0004-6361:20041335

Lippold, J., Gherardi, J.-M., & Luo, Y. (2011). Testing the 231Pa/230Th paleocirculation proxy: A data versus 2D model comparison. *Geophysical Research Letters*, *38*, L20603. https://doi.org/10.1029/2011GL049282

Lippold, J., Gutjahr, M., Blaser, P., Christner, E., de Carvalho Ferreira, M. L., Mulitza, S., et al. (2016). Deep water provenance and dynamics of the (de)glacial Atlantic Meridional Overturning Circulation. *Earth and Planetary Science Letters*, *445*, 68–78. https://doi.org/10.1016/J.EPSL.2016.04.013

Lippold, J., Luo, Y., François, R., Allen, S. E., Gherardi, J., Pichat, S., et al. (2012a). Strength and geometry of the glacial Atlantic Meridional Overturning Circulation. *Nature Geoscience*, *5*(11), 813–816. https://doi.org/10.1038/ngeo1608

Lippold, J., Mulitza, S., Mollenhauer, G., Weyer, S., Heslop, D., & Christl, M. (2012b). Boundary scavenging at the East Atlantic margin does not negate use of 231Pa/230Th to trace Atlantic overturning. *Earth and Planetary Science Letters*, *333–334*, 317–331. https://doi.org/10.1016/j.epsl.2012.04.005

Lund, D. C., Pavia, F. J., Seeley, E. I., McCart, S. E., Rafter, P. A., Farley, K. A., et al. (2019). Hydrothermal scavenging of 230Th on the Southern East Pacific Rise during the last deglaciation. *Earth and Planetary Science Letters*, *510*, 64–72. https://doi.org/10.1016/j.epsl.2018.12.037

Maher, B. A., Prospero, J. M., Mackie, D., Gaiero, D., Hesse, P. P., & Balkanski, Y. (2010). Global connections between aeolian dust, climate and ocean biogeochemistry at the present day and at the last glacial maximum. *Earth-Science Reviews*, *99*(1–2), 61–97. https://doi.org/10.1016/j.earscirev.2009.12.001

Mahowald, N. M., Baker, A. R., Bergametti, G., Brooks, N., Duce, R. A., Jickells, T. D., et al. (2005). Atmospheric global dust cycle and iron inputs to the ocean. *Global Biogeochemical Cycles*, *19*, GB4025. https://doi.org/10.1029/2004GB002402

Marshall, J., Donohoe, A., Ferreira, D., & McGee, D. (2014). The ocean's role in setting the mean position of the Inter-Tropical Convergence Zone. *Climate Dynamics*, *42*(7–8), 1967–1979. https://doi.org/10.1007/s00382-013-1767-z

McGee, D. (2020). Glacial-interglacial precipitation changes. *Annual Review of Marine Science*, *12*(1), 525–557. https://doi.org/10.1146/annurev-marine-010419-010859

McGee, D., Broecker, W. S., & Winckler, G. (2010a). Gustiness: The driver of glacial dustiness? *Quaternary Science Reviews*, *29*(17–18), 2340–2350. https://doi.org/10.1016/j.quascirev.2010.06.009

McGee, D., DeMenocal, P. B. B., Winckler, G., Stuut, J. B. W., & Bradtmiller, L. I. (2013). The magnitude, timing and abruptness of changes in North African dust deposition over the last 20,000 yr. *Earth and Planetary Science Letters*, *371–372*, 163–176. https://doi.org/10.1016/J.EPSL.2013.03.054

McGee, D., Donohoe, A., Marshall, J., & Ferreira, D. (2014). Changes in ITCZ location and cross-equatorial heat transport at the Last Glacial Maximum, Heinrich Stadial 1, and the mid-Holocene. *Earth and Planetary Science Letters*, *390*, 69–79. https://doi.org/10.1016/j.epsl.2013.12.043

McGee, D., Marcantonio, F., & Lynch-Stieglitz, J. (2007). Deglacial changes in dust flux in the eastern equatorial Pacific. *Earth and Planetary Science Letters*, *257*(1–2), 215–230. https://doi.org/10.1016/J.EPSL.2007.02.033

McGee, D., Marcantonio, F., McManus, J. F., & Winckler, G. (2010b). The response of excess 230Th and extraterrestrial 3He to sediment redistribution at the Blake Ridge, western North Atlantic. *Earth and Planetary Science Letters*, *299*, 138–149. https://doi.org/10.1016/j.epsl.2010.08.029

McGee, D., Winckler, G., Borunda, A., Serno, S., Anderson, R. F., Recasens, C., et al. (2016). Tracking eolian dust with helium and thorium: Impacts of grain size and provenance. *Geochimica et Cosmochimica Acta*, *175*, 47–67. https://doi.org/10.1016/j.gca.2015.11.023

Meckler, A. N., Sigman, D. M., Gibson, K. A., François, R., Martínez-García, A., Jaccard, S. L., et al. (2013). Deglacial pulses of deep-ocean silicate into the subtropical North Atlantic Ocean. *Nature*, *495*(7442), 495–498. https://doi.org/10.1038/nature12006

Mekik, F., & Anderson, R. F. (2018). Is the core top modern? Observations from the eastern equatorial Pacific. *Quaternary Science Reviews*, *186*, 156–168. https://doi.org/10.1016/j.quascirev.2018.01.020

Middleton, J. L., Langmuir, C. H., Mukhopadhyay, S., McManus, J. F., & Mitrovica, J. X. (2016). Hydrothermal iron flux variability following rapid sea level changes. *Geophysical Research Letters*, *43*, 3848–3856. https://doi.org/10.1002/2016GL068408

Middleton, J. L., Mukhopadhyay, S., Costa, K. M., Pavia, F. J., Winckler, G., McManus, J. F., et al. (2020). The spatial footprint of hydrothermal scavenging on 230ThXS-derived mass accumulation rates. *Geochimica et Cosmochimica Acta*, *272*, 218–234. https://doi.org/10.1016/J.GCA.2020.01.007

Middleton, J. L., Mukhopadhyay, S., Langmuir, C. H., McManus, J. F., & Huybers, P. J. (2018). Millennial-scale variations in dustiness recorded in Mid-Atlantic sediments from 0 to 70 ka. *Earth and Planetary Science Letters*, *482*, 12–22. https://doi.org/10.1016/J.EPSL.2017.10.034

Missiaen, L., Pichat, S., Waelbroeck, C., Douville, E., Bordier, L., Dapoigny, A., et al. (2018). Downcore variations of sedimentary detrital (238U/232Th) ratio: Implications on the use of 230Thxs and 231Paxs to reconstruct sediment flux and ocean circulation. *Geochemistry, Geophysics, Geosystems*, *19*, 2560–2573. https://doi.org/10.1029/2017GC007410

Moore, C. M., Mills, M. M., Achterberg, E. P., Geider, R. J., LaRoche, J., Lucas, M. I., et al. (2009). Large-scale distribution of Atlantic nitrogen fixation controlled by iron availability. *Nature Geoscience*, *2*(12), 867–871. https://doi.org/10.1038/ngeo667

Moore, C. M., Mills, M. M., Arrigo, K. R., Berman-Frank, I., Bopp, L., Boyd, P. W., et al. (2013). Processes and patterns of oceanic nutrient limitation. *Nature Geoscience*, *6*(9), 701–710. https://doi.org/10.1038/ngeo1765

Muhs, D. R., Budahn, J. R., Prospero, J. M., & Carey, S. N. (2007). Geochemical evidence for African dust inputs to soils of western Atlantic islands: Barbados, the Bahamas, and Florida. *Journal of Geophysical Research*, *112*, F02009. https://doi.org/10.1029/2005JF000445

Mulitza, S., Chiessi, C. M., Schefuß, E., Lippold, J., Wichmann, D., Antz, B., et al. (2017). Synchronous and proportional deglacial changes in Atlantic meridional overturning and northeast Brazilian precipitation. *Paleoceanography*, *32*, 622–633. https://doi.org/10.1002/2017PA003084

Mulitza, S., Prange, M., Stuut, J.-B., Zabel, M., von Dobeneck, T., Itambi, A. C., et al. (2008). Sahel megadroughts triggered by glacial slowdowns of Atlantic meridional overturning. *Paleoceanography*, *23*, PA4206. https://doi.org/10.1029/2008PA001637

Muller, J., McManus, J. F., Oppo, D. W., & Francois, R. (2012). Strengthening of the Northeast Monsoon over the Flores Sea, Indonesia, at the time of Heinrich event 1. *Geology*, *40*(7), 635–638. https://doi.org/10.1130/G32878.1

Neuer, S., Ratmeyer, V., Davenport, R., Fischer, G., & Wefer, G. (1997). Deep water particle flux in the Canary Island region: Seasonal trends in relation to long-term satellite derived pigment data and lateral sources. *Deep Sea Research Part I: Oceanographic Research Papers*, *44*(8), 1451–1466. https://doi.org/10.1016/S0967-0637(97)00034-4

Ng, H. C., Robinson, L. F., McManus, J. F., Mohamed, K. J., Jacobel, A. W., Ivanovic, R. F., et al. (2018). Coherent deglacial changes in western Atlantic Ocean circulation. *Nature Communications*, *9*(1), 2947. https://doi.org/10.1038/s41467-018-05312-3

Nicholson, S. E. (2009). A revised picture of the structure of the "monsoon" and land ITCZ over West Africa. *Climate Dynamics*, *32*(7–8), 1155–1171. https://doi.org/10.1007/s00382-008-0514-3

Pabortsava, K., Lampitt, R. S., Benson, J., Crowe, C., McLachlan, R., Le Moigne, F. A. C., et al. (2017). Carbon sequestration in the deep Atlantic enhanced by Saharan dust. *Nature Geoscience*, *10*(3), 189–194. https://doi.org/10.1038/ngeo2899

Peters, M., & Tetzlaff, G. (1990). West African palaeosynoptic ptterns at the Last Glacial Maximum. *Theoretical and Applied Climatology*, *42*, 67–79. https://doi.org/10.1007/BF00865527

Peucker-Ehrenbrink, B. (2009). Land2Sea database of river drainage basin sizes, annual water discharges, and suspended sediment fluxes. *Geochemistry, Geophysics, Geosystems*, *10*, Q06014. https://doi.org/10.1029/2008GC002356

Peucker-Ehrenbrink, B. (2018). *Land2Sea database, Version 2.0.*, PANGAEA. https://doi.org/10.1594/PANGAEA.892680

Portilho-Ramos, R. C., Chiessi, C. M., Zhang, Y., Mulitza, S., Kucera, M., Siccha, M., et al. (2017). Coupling of equatorial Atlantic surface stratification to glacial shifts in the tropical rainbelt. *Scientific Reports*, *7*(1), 1561. https://doi.org/10.1038/s41598-017-01629-z

Pourmand, A., Marcantonio, F., & Schulz, H. (2004). Variations in productivity and eolian fluxes in the northeastern Arabian Sea during the past 110 ka. *Earth and Planetary Science Letters*, *221*(1–4), 39–54. https://doi.org/10.1016/S0012-821X(04)00109-8

Prospero, J. M., & Carlson, T. N. (1980). Saharan air outbreaks over the tropical North Atlantic. *Pure and Applied Geophysics*, *119*, 677–691. https://doi.org/10.1007/BF00878167

Prospero, J. M., Ginoux, P., Torres, O., Nicholson, S. E., & Gill, T. E. (2002). Environmental characterization of global sources of atmospheric soil dust identified with the NIMBUS 7 Total Ozone Mapping Spectrometer (TOMS) absorbing aerosol product. *Reviews of Geophysics*, *40*(1), 1002. https://doi.org/10.1029/2000RG000095

Pye, K. (1987). *Aeolian dust and dust deposits*. London: Academic Press.

Ratmeyer, V., Fischer, G., & Wefer, G. (1999). Lithogenic particle fluxes and grain size distributions in the deep ocean off northwest Africa: Implications for seasonal changes of aeolian dust input and downward transport. *Deep-Sea Research Part I: Oceanographic Research Papers*, *46*(8), 1289–1337. https://doi.org/10.1016/S0967-0637(99)00008-4

Reimi, M. A., Marcantonio, F., Lynch-Stieglitz, J., Jacobel, A. W., McManus, J. F., & Winckler, G. (2019). The penultimate glacial termination and variability of the Pacific intertropical convergence zone. *Geophysical Research Letters*, *46*, 4826–4835. https://doi.org/10.1029/2018GL081403

Ridley, D. A., Heald, C. L., & Ford, B. (2012). North African dust export and deposition: A satellite and model perspective. *Journal of Geophysical Research*, *117*, D02202. https://doi.org/10.1029/2011JD016794

Rowland, G. H., Ng, H. C., Robinson, L. F., McManus, J. F., Mohamed, K. J., & McGee, D. (2017). Investigating the use of 232Th/230Th as a dust proxy using co-located seawater and sediment samples from the low-latitude North Atlantic. *Geochimica et Cosmochimica Acta*, *214*, 143–156. https://doi.org/10.1016/j.gca.2017.07.033

Ruddiman, W. F. (1997). Tropical Atlantic terrigenous fluxes since 25,000 yrs B.P. *Marine Geology*, *136*(3–4), 189–207. https://doi.org/10.1016/S0025-3227(96)00069-2

Rudnick, R. L., & Gao, S. (2003). Composition of the continental crust. *Treatise on Geochemistry*, *3*, 1–64. https://doi.org/10.1016/B0-08-043751-6/03016-4

Rühlemann, C., Diekmann, B., Mulitza, S., & Frank, M. (2001). Late Quaternary changes of western equatorial Atlantic surface circulation and Amazon lowland climate recorded in Ceará Rise deep-sea sediments. *Paleoceanography*, *16*(3), 293–305. https://doi.org/10.1029/1999PA000474

Sarnthein, M., Tetzlaff, G., Koopmann, B., Wolter, K., & Pflaumann, U. (1981). Glacial and interglacial wind regimes over the eastern subtropical Atlantic and North-West Africa. *Nature*, *293*(5829), 193–196. https://doi.org/10.1038/293193a0

Scheff, J., Seager, R., Liu, H., & Coats, S. (2017). Are glacials dry? Consequences for paleoclimatology and for greenhouse warming. *Journal of Climate*, *30*(17), 6593–6609. https://doi.org/10.1175/JCLI-D-16-0854.1

Schepanski, K., Tegen, I., & Macke, A. (2009a). Saharan dust transport and deposition towards the tropical northern Atlantic. *Atmospheric Chemistry and Physics*, *9*, 1173–1189 https://doi.org/10.5194/acp-9-1173-2009

Schepanski, K., Tegen, I., Todd, M. C., Heinold, B., Bönisch, G., Laurent, B., & Macke, A. (2009b). Meteorological processes forcing Saharan dust emission inferred from MSG-SEVIRI observations of subdaily dust source activation and numerical models. *Journal of Geophysical Research*, *114*, D10201. https://doi.org/10.1029/2008JD010325

Schlitzer, R (2018). Ocean Data View. https://odv.awi.de

Schlosser, C., Klar, J. K., Wake, B. D., Snow, J. T., Honey, D. J., Woodward, E. M. S., et al. (2014). Seasonal ITCZ migration dynamically controls the location of the (sub)tropical Atlantic biogeochemical divide. *Proceedings of the National Academy of Sciences of the United States of America*, *111*(4), 1438–1442. https://doi.org/10.1073/pnas.1318670111

Schmid, C., Molinari, R. L., & Garzoli, S. L. (2001). New observations of the intermediate depth circulation in the tropical Atlantic. *Journal of Marine Research*, *59*(2), 281–312. https://doi.org/10.1357/002224001762882664

Schneider, T., Bischoff, T., & Haug, G. H. (2014). Migrations and dynamics of the intertropical convergence zone. *Nature*, *513*(7516), 45–53. https://doi.org/10.1038/nature13636

Schütz, L. (1980). Long range transport of desert dust with special emphasis on the Sahara. *Annals of the New York Academy of Sciences*, *338*(1), 515–532. https://doi.org/10.1111/j.1749-6632.1980.tb17144.x

Singarayer, J. S., Valdes, P. J., & Roberts, W. H. G. (2017). Ocean dominated expansion and contraction of the late Quaternary tropical rainbelt. *Scientific Reports*, *7*(1), 9382. https://doi.org/10.1038/s41598-017-09816-8

Skonieczny, C., McGee, D., Winckler, G., Bory, A., Bradtmiller, L. I., Kinsley, C. W., et al. (2019). Monsoon-driven Saharan dust variability over the past 240,000 years. *Science Advances*, *5*(1), eaav1887. https://doi.org/10.1126/sciadv.aav1887

Stríkis, N. M., Cruz, F. W., Barreto, E. A. S., Naughton, F., Vuille, M., Cheng, H., et al. (2018). South American monsoon response to iceberg discharge in the North Atlantic. *Proceedings of the National Academy of Sciences of the United States of America*, *115*(15), 3788–3793. https://doi.org/10.1073/pnas.1717784115

Strong, J. D. O., Vecchi, G. A., Ginoux, P., Strong, J. D. O., Vecchi, G. A., & Ginoux, P. (2015). The response of the tropical Atlantic and West African Climate to Saharan dust in a fully coupled GCM. *Journal of Climate*, *28*(18), 7071–7092. https://doi.org/10.1175/JCLI-D-14-00797.1

Taylor, S. R., & McLennan, S. M. (1995). The geochemical evolution of the continental crust. *Reviews of Geophysics*, *33*(2), 241. https://doi.org/10.1029/95RG00262

Trauth, M. H., Sarnthein, M., & Arnold, M. (1997). Bioturbational mixing depth and carbon flux at the seafloor. *Paleoceanography*, *12*(3), 517–526. https://doi.org/10.1029/97PA00722

van der Does, M., Brummer, G. J. A., van Crimpen, F. C. J., Korte, L. F., Mahowald, N. M., Merkel, U., et al. (2020). Tropical rains controlling deposition of Saharan dust across the North Atlantic Ocean. *Geophysical Research Letters*, *47*, e2019GL086867. https://doi.org/10.1029/2019GL086867

van der Jagt, H., Friese, C., Stuut, J.-B. W., Fischer, G., & Iversen, M. H. (2018). The ballasting effect of Saharan dust deposition on aggregate dynamics and carbon export: Aggregation, settling, and scavenging potential of marine snow. *Limnology and Oceanography*, *63*(3), 1386–1394. https://doi.org/10.1002/lno.10779

Voigt, I., Cruz, A. P. S., Mulitza, S., Chiessi, C. M., Mackensen, A., Lippold, J., et al. (2017). Variability in mid-depth ventilation of the western Atlantic Ocean during the last deglaciation. *Paleoceanography*, *32*, 948–965. https://doi.org/10.1002/2017PA003095

Waelbroeck, C., Pichat, S., Böhm, E., Lougheed, B. C., Faranda, D., Vrac, M., et al. (2018). Relative timing of precipitation and ocean circulation changes in the western equatorial Atlantic over the last 45 kyr. *Climate of the Past*, *14*, 1315–1330. https://doi.org/10.5194/cp-14-1315-2018

Wang, X., Auler, A. S., Edwards, R. L., Cheng, H., Ito, E., & Solheid, M. (2006). Interhemispheric anti-phasing of rainfall during the last glacial period. *Quaternary Science Reviews*, *25*(23–24), 3391–3403. https://doi.org/10.1016/J.QUASCIREV.2006.02.009

Washington, R., Todd, M. C., Lizcano, G., Tegen, I., Flamant, C., Koren, I., et al. (2006). Links between topography, wind, deflation, lakes and dust: The case of the Bodélé Depression, Chad. *Geophysical Research Letters*, *33*, L09401. https://doi.org/10.1029/2006GL025827

Williams, R. H., McGee, D., Kinsley, C. W., Ridley, D. A., Hu, S., Fedorov, A., et al. (2016). Glacial to Holocene changes in trans-Atlantic Saharan dust transport and dust-climate feedbacks. *Science Advances*, *2*(11), e1600445. https://doi.org/10.1126/sciadv.1600445

Winckler, G., Anderson, R. F., Fleisher, M. Q., McGee, D., & Mahowald, N. (2008). Covariant glacial-interglacial dust fluxes in the Equatorial Pacific and Antarctica. *Science*, *320*(5872), 93–96. https://doi.org/10.1126/science.1150595

Wu, C., Lin, Z., & Liu, X. (2020). The global dust cycle and uncertainty in CMIP5 (Coupled Model Intercomparison Project phase 5) models. *Atmospheric Chemistry and Physics*, *20*(17), 10401–10425. https://doi.org/10.5194/acp-20-10401-2020

Wu, M. C., Reale, O., Schubert, S. D., Suarez, M. J., Koster, R. D., & Pegion, P. J. (2009). African Easterly Jet: Structure and maintenance. *Journal of Climate*, *22*(17), 4459–4480. https://doi.org/10.1175/2009JCLI2584.1

Wynn, R. B., Weaver, P. P. E., Masson, D. G., & Stow, D. A. V. (2002). Turbidite depositional architecture across three interconnected deep-water basins on the north-west African margin. *Sedimentology*, *49*(4), 669–695. https://doi.org/10.1046/j.1365-3091.2002.00471.x

Yu, E. F., Francois, R., Bacon, M. P., & Fleer, A. P. (2001). Fluxes of 230Th and 231Pa to the deep sea: Implications for the interpretation of excess 230Th and 231Pa/230Th profiles in sediments. *Earth and Planetary Science Letters*, *191*(3–4), 219–230. https://doi.org/10.1016/S0012-821X(01)00410-1

Yu, H., Chin, M., Bian, H., Yuan, T., Prospero, J. M., Omar, A. H., et al. (2015). Quantification of trans-Atlantic dust transport from seven-year (2007–2013) record of CALIPSO lidar measurements. *Remote Sensing of Environment*, *159*, 232–249. https://doi.org/10.1016/j.rse.2014.12.010

Yu, H., Tan, Q., Chin, M., Remer, L. A., Kahn, R. A., Bian, H., et al. (2019). Estimates of African dust deposition along the trans-Atlantic transit using the decadelong record of aerosol measurements from CALIOP, MODIS, MISR, and IASI. *Journal of Geophysical Research: Atmospheres*, 124, 7975–7996. https://doi.org/10.1029/2019JD030574

Zabel, M., Bickert, T., Dittert, L., & Haese, R. R. (1999). Significance of the sedimentary Al:Ti ratio as an indicator for variations in the circulation patterns of the equatorial North Atlantic. *Paleoceanography*, *14*(6), 789–799. https://doi.org/10.1029/1999PA900027

Zhang, D., McPhaden, M. J., & Johns, W. E. (2003). Observational evidence for flow between the subtropical and tropical Atlantic: The Atlantic subtropical cells. *Journal of Physical Oceanography*, *33*(8), 1783–1797. https://doi.org/10.1175/1520-0485(2003)033<1783:OEFFBT>2.0.CO;2

Zhang, Y., Chiessi, C. M., Mulitza, S., Zabel, M., Trindade, R. I. F., Hollanda, M. H. B. M., et al. (2015). Origin of increased terrigenous supply to the NE South American continental margin during Heinrich Stadial 1 and the Younger Dryas. *Earth and Planetary Science Letters*, *432*, 493–500. https://doi.org/10.1016/j.epsl.2015.09.054